EXOTICS SEARCHES AT ATLAS*

Erich W. Varnes

on behalf of the ATLAS Collaboration

Department of Physics, University of Arizona
1118 E. Fourth Street, PO Box 210081, Tucson, AZ 85721, USA

(Received April 28, 2016)

A broad range of searches for exotic phenomena has been carried out at the ATLAS experiment at the Large Hadron Collider, using 3.2 fb^{-1} of pp collisions at $\sqrt{s} = 13$ TeV. These searches did not uncover any discrepancies with the Standard Model.

DOI:10.5506/APhysPolB.47.1595

1. Introduction

The search for phenomena beyond the Standard Model (BSM) is one of the primary motivations for the physics program at the Large Hadron Collider (LHC). The presence of dark matter in the universe and the hierarchy problem provide strong hints that new phenomena should exist. The increase of the LHC energy from 8 to 13 TeV in 2015 greatly extended the capacity of the LHC to produce new particles in pp collisions. In these Proceedings, results from searches for exotic particles using ≈ 3 fb^{-1} of data collected by ATLAS detector [1] are presented, where 'exotic' means BSM particles outside of the framework of supersymmetry, and also not including BSM Higgs bosons (searches for such particles are reported elsewhere in these proceedings).

2. Diboson searches

Many new physics models predict the existence of heavy particles that decay into a pair of bosons. Searches for diboson resonances are performed in a variety of final states, and the results are interpreted in the context of several models, including the 'Heavy Vector Triplet' (HVT) formulation of Ref. [2], which allows translation to a broad set of models.

* Presented at the Cracow Epiphany Conference on the Physics in LHC Run 2, Kraków, Poland, January 7–9, 2016.

2.1. Hadronic boson tagging

The data from the 2010–2012 run of the LHC indicate that if new resonances that decay to dibosons exist, the masses of these resonances must be much greater than the W/Z boson masses. This means that the W or Z bosons in the final state will tend to be highly boosted in the lab frame, so that hadronic decays of these Ws and Zs will tend to result in jets that overlap in the calorimeter. To identify these collimated decays, jets from energy deposits in the calorimeter are reconstructed using the anti-k_{t} algorithm [3–5] with a radius parameter R of 1.0. If this large jet arises from two separate quarks, the pattern of energy deposition within the jet reflects this. To extract this information, first the jets are 'trimmed' by removing low-p_{T} $R = 0.2$ subjets within the large jet. A requirement is then placed on the ratio of the energy correlations of the remaining subjets. The jets that satisfy this criterion are considered to be 'W-tagged' ('Z-tagged') if their mass is within 15 GeV of the W (Z) boson mass, and are generically denoted as J. Details of the hadronic boson tagging procedure are available in Refs. [6, 7]. Figure 1 demonstrates the ability of this method to identify hadronically-decaying vector bosons above the QCD background.

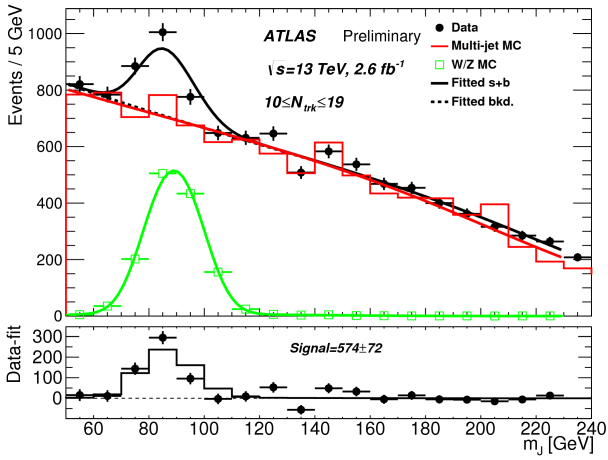

Fig. 1. (Color online) The mass distribution of large-R jets for events with between 10 and 19 reconstructed tracks associated with the leading jet. In the top panel, light gray (green) is for the $W+Z$ simulation and its signal shape fit and gray (red) is the multi-jet background and a background-only fit. Data is shown in black, with a solid line for the signal plus background fit and a dotted black line which is the background-only component of that fit. The lower panel shows the data and the total fit with the background component of the fit subtracted [8].

2.2. Search for $WW/WZ/ZZ \to qq$

The search for hadronically-decaying boson pairs is of special interest since the ATLAS Run 1 data revealed an excess at the 3.5σ level near $m_{JJ} = 2$ TeV (the corresponding global significance was 2.5σ) [9]. The m_{JJ} distribution for the Run 2 data is shown in figure 2 [8]. No excess appears near 2 TeV, but more data is required before conclusions can be drawn.

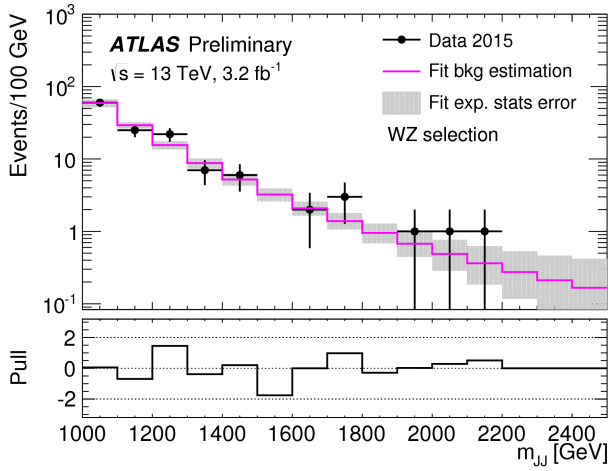

Fig. 2. The observed data in the signal regions of the WZ channel. Also shown is the fitted background. The region in gray represents the uncertainty on the background estimate due to the fit [8].

2.3. Search for $ZZ/WZ \to \ell\ell qq$

The diboson final state with a Z boson decaying leptonically and a W or Z boson decaying hadronically has also been investigated [10]. The W boson is identified via a tagged jet, while the lepton pair is required to satisfy 83 GeV $< m_{ee} <$ 99 GeV or 66 GeV $< m_{\mu^{\pm}\mu^{\mp}} <$ 116 GeV, with the differences reflecting the better mass resolution in the electron channel and the fact that there is a non-negligible probability for the charge of an electron to be mismeasured. The $\ell\ell J$ mass distributions are shown in figure 3. Good agreement is found between the data and the background expectation; the resulting limit in the context of the HVT model is shown in figure 4.

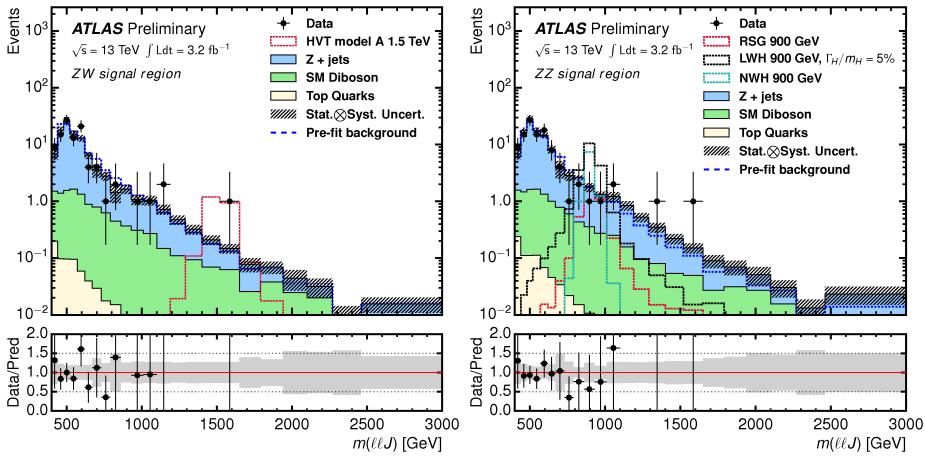

Fig. 3. Comparisons of the observed and expected $m_{\ell\ell J}$ distributions for (left) the ZW and (right) the ZZ signal regions combining the eeJ and $\mu\mu J$ final states. The last bin includes overflows. Distributions for some of the signals this search is sensitive to are also shown. The bottom panel shows the ratio of the observed data to the predicted background [10].

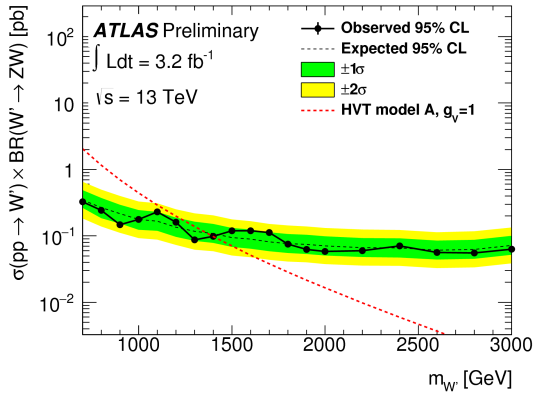

Fig. 4. Observed and expected 95% C.L. upper limits on $\sigma\times$ BR for a HVT W' resonance decaying to a WZ pair as a function of the resonance mass. The theoretical cross section for a HVT Model A W' is also shown [10].

2.4. Search for $WW/WZ \to \ell\nu qq$

Complementary to the ZZ/WZ search described above, this search explores the case where one W boson decays leptonically and the other boson in the event decays hadronically [11]. The invariant mass of the diboson system is computed by using the W mass constraint to solve for the p_z of the

neutrino (with the solution with the smaller $|p_z|$ value being taken). The $\ell\nu J$ mass distributions in the WW and WZ signal regions are shown in figure 5. Good agreement is found between the data and the background expectation; the resulting limit in the context of the HVT model and a Graviton model are shown in figure 6.

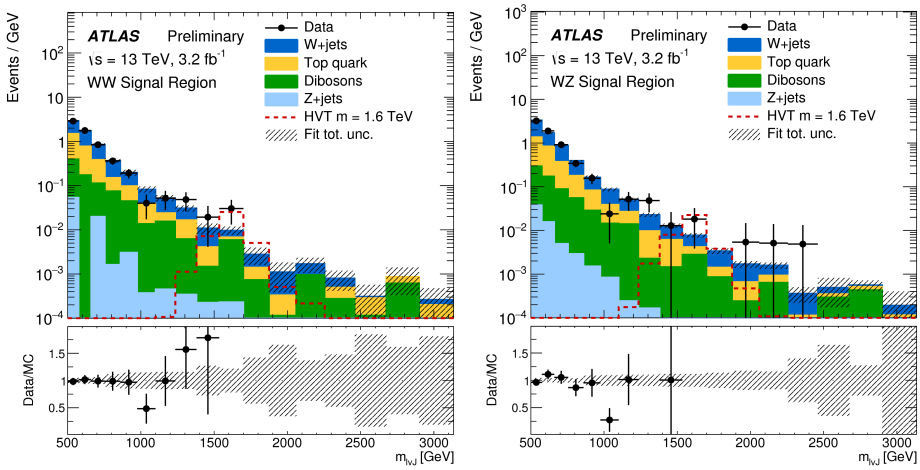

Fig. 5. Reconstructed $m_{\ell\nu J}$ distributions in data and the predicted background in the (left) WW signal region and (right) WZ signal region. The band denotes the statistical and systematic uncertainty on the background. The lower panels show the ratio of data to the SM background estimate [11].

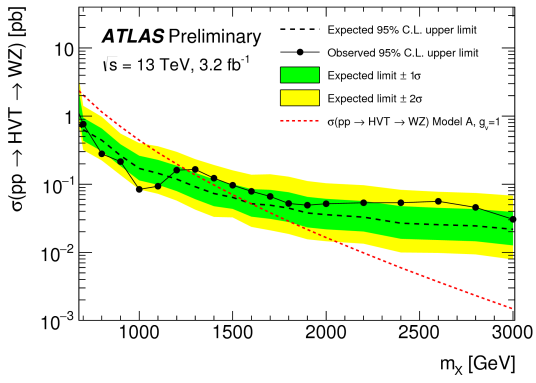

Fig. 6. Observed and expected 95% C.L. upper limits on the production cross section times branching ratio of an HVT and a Graviton as a function of the resonance mass. The theoretical cross sections for the HVT and Graviton benchmark resonance model are shown [11].

2.5. Search for $WZ/ZZ \to \nu\nu qq$

The final search for anomalous production of vector boson pairs considers the case where a Z boson decays to $\nu\nu$, while the other boson in the event decays hadronically [12]. The signature in this case is a single $R = 1.0$ jet recoiling against substantial missing transverse momentum, and the distribution of the transverse mass formed from the missing transverse momentum and the jet is compared to the SM expectation. The results for the WZ and ZZ signal regions are shown in figure 7. As with the other diboson searches, good agreement with the SM expectation is observed. The resulting limits in the context of the HVT model are shown in figure 8.

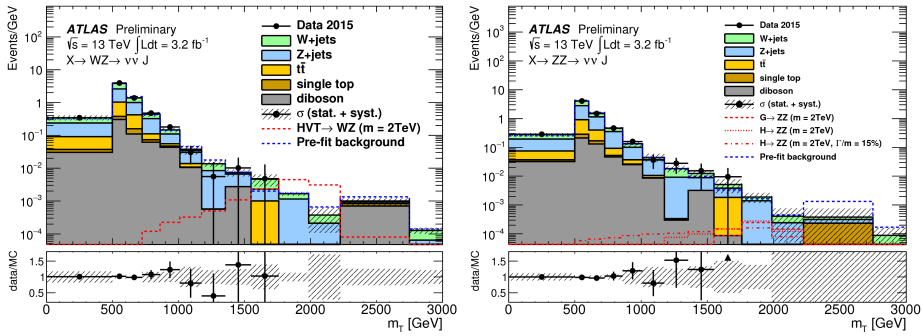

Fig. 7. Comparison of data to the expected Standard Model background for the transverse mass (m_{T}) spectrum in (left) the WZ signal region and (right) the ZZ signal region [12].

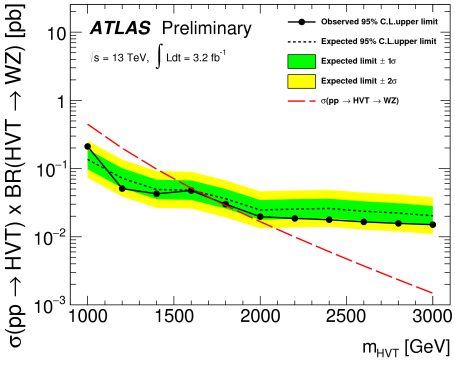

Fig. 8. (Color online) The expected and observed 95% confidence level upper limits on production cross section ($\sigma(pp \to \mathrm{HVT})$) times branching fraction ($\mathrm{BR}(\mathrm{HVT} \to WZ)$) for the benchmark Heavy Vector Triplet model. The theoretical prediction for the signal cross section is shown by the dashed (red) line [12].

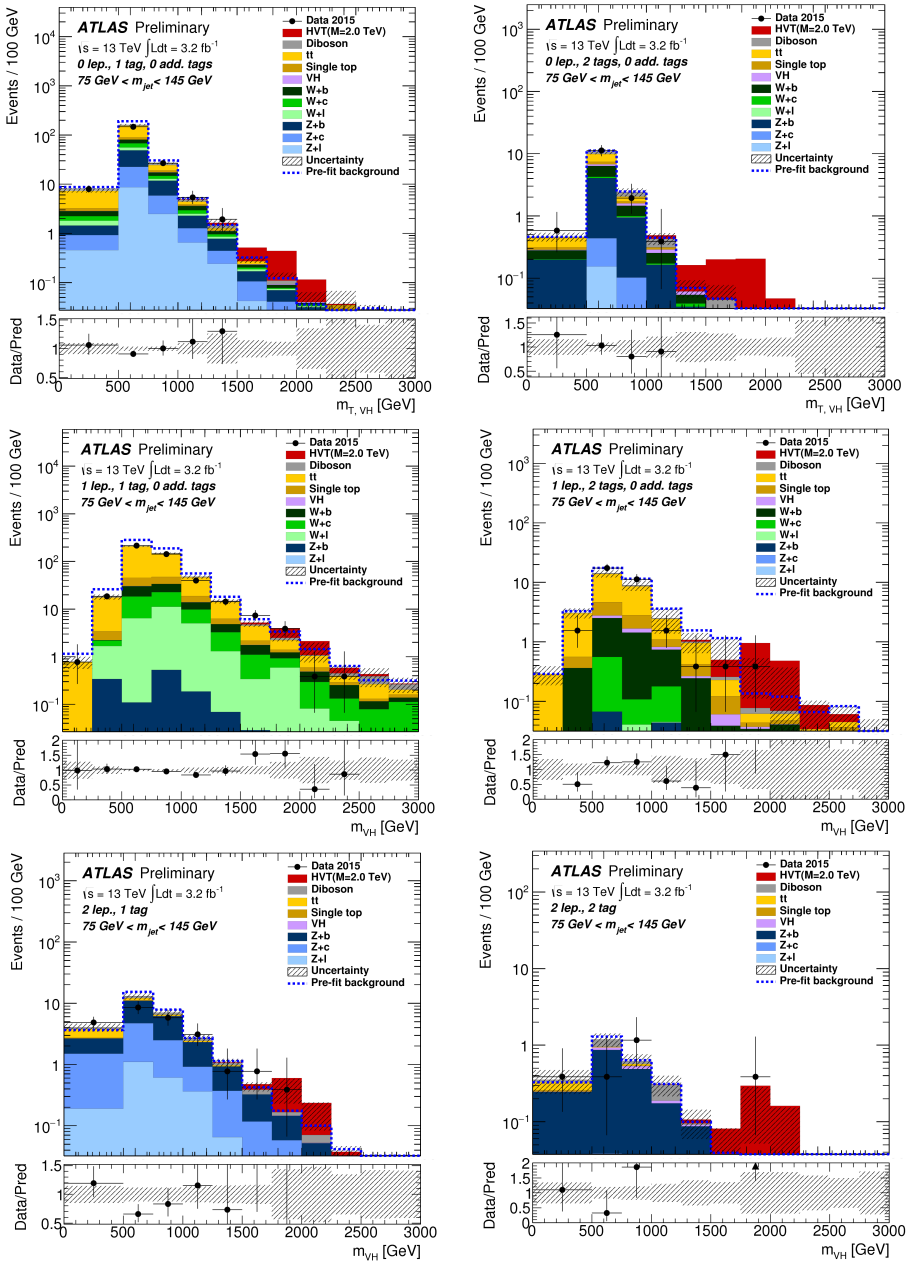

Fig. 9. Distributions of m_{T}, VH and m_{VH} for the (top) 0-, (middle) 1-, and (bottom) 2-lepton channels. The left (right) column corresponds to the 1-b-tag (2-b-tag) signal regions. The signal for the benchmark HVT Model A with m'_V = 2000 GeV is shown stacked on top of the background and normalized to the expected 95% C.L. upper cross-section limit [13].

2.6. Search for $W/Z + H \to (\nu\nu\ /\ell\nu/\ell\ell)b\bar{b}$

Another variant of the search for a resonance decaying to a pair of bosons covers the case where one of the bosons is a W or Z and the other is a Higgs [13]. The Higgs boson is sought using its $b\bar{b}$ decay, while all leptonic decays of the vector boson are considered. This leads to three distinct final state signatures ($\nu\nu b\bar{b}$, $\ell\nu b\bar{b}$, and $\ell\ell b\bar{b}$). In addition, events with one and two b-tagged jets are treated separately to maximize the sensitivity of the search. For the $\nu\nu b\bar{b}$ channel, the distribution of the transverse mass of the jets and missing transverse momentum are compared to the SM expectation; for the other channels, the invariant mass of the diboson system is compared. The results are shown in figure 9, with no significant excess in data observed.

3. Search for dark matter produced in association with a W/Z boson

The existence of dark matter (DM) provides one of the strongest motivations for searches for exotic particles at the LHC. If the DM particle (called χ) is produced in association with a W or Z boson that decays hadronically, the resulting signature will be a boson-tagged jet recoiling against large missing transverse momentum. A search for this signature has been performed, where the missing transverse momentum of the selected events is compared to the expectation from the SM [14]. This comparison, shown in figure 10, reveals no significant discrepancy. The result is

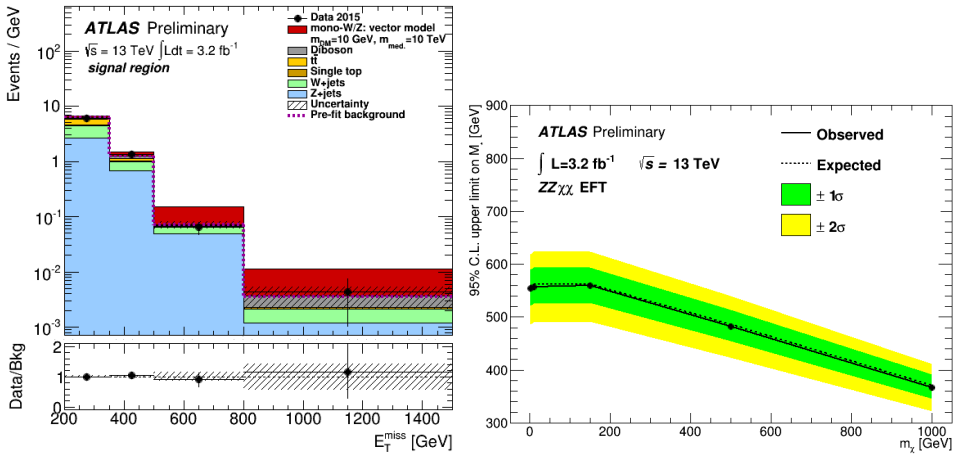

Fig. 10. Left: The $E_{\mathrm{T}}^{\mathrm{miss}}$ distribution of the events in the signal region. The inset at the bottom of the plot shows the ratio of the data to the total background. Right: The limit on the mass scale, $M_\star$, of the $ZZ\chi\chi$ [14].

interpreted in the context of an effective $ZZ\chi\chi$ coupling, and also in a model where the production is mediated by a new vector boson. Limits under the $ZZ\chi\chi$ scenario are shown in figure 10.

4. Searches in the dijet final state

Any new particle that can be created at the LHC must couple to quarks or gluons, and, therefore, searches using the dijet final state have broad sensitivity to new physics. Two variables are used for these searches [15]: *(i)* the dijet invariant mass m_{jj} which is sensitive to new particles in the s-channel, and *(ii)* $\chi \equiv \exp(|y_1 - y_2|)$, where y_1 and y_2 are the rapidities of the jets, which is sensitive to new particles in the t-channel. The m_{jj} distribution is shown in figure 11 (left), and the resulting limits on the cross section for a generic Gaussian dijet resonance are shown in figure 11 (right). The distributions of the χ variable, in different m_{jj} regions, are shown in figure 12. In all cases, good agreement with the SM expectation is observed.

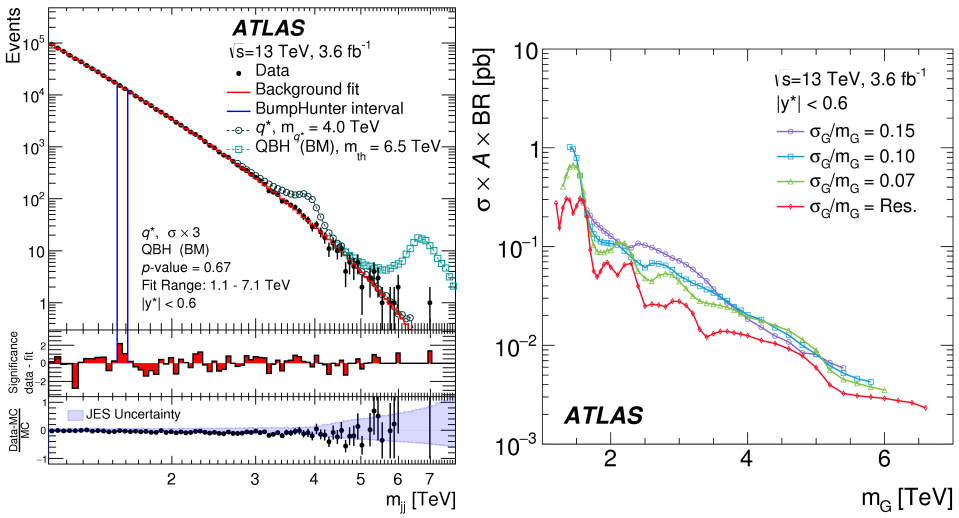

Fig. 11. Left panel: The reconstructed dijet mass distribution (filled points) for events with $|y^\star| < 0.6$ and $p_T > 440$ (50) GeV for the leading (subleading) jets. The solid line depicts the fit to an empirical background distribution function. Predictions for an excited quark and a quantum black hole are also shown. The vertical lines indicate the most interval with the largest discrepancy. The middle panel shows the bin-by-bin significances of the data–fit differences. The lower panel shows the relative differences between the data and the prediction of PYTHIA 8 simulation. Right panel: The 95% credibility-level upper limits obtained from the m_{jj} distribution on cross section times acceptance times branching ratio to two jets for a hypothetical signal that is Gaussian in m_{jj}, with various widths, as a function of the mean mass of the Gaussian distribution, m_G [15].

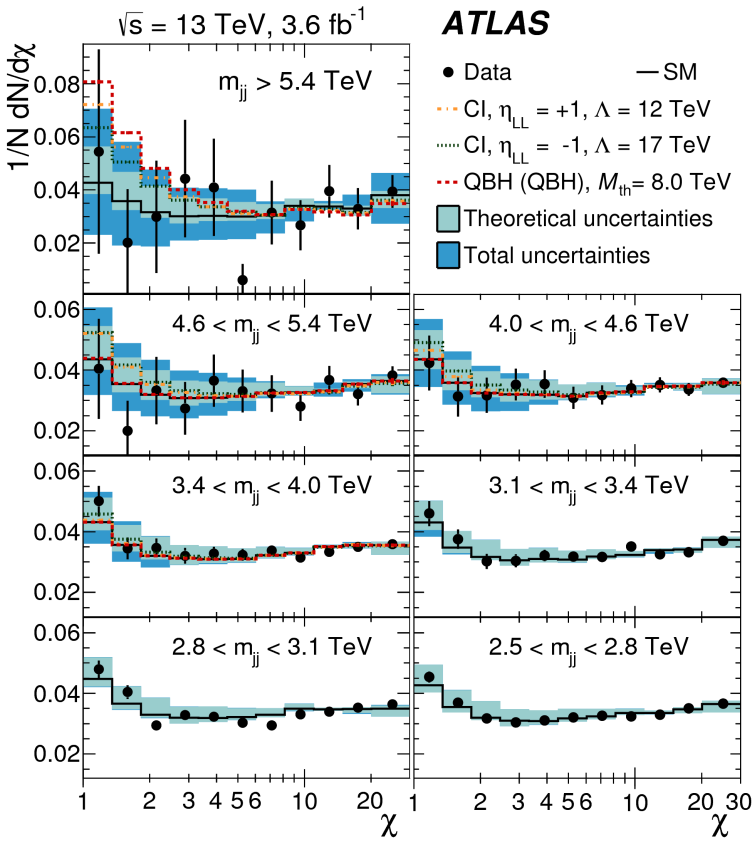

Fig. 12. Reconstructed distributions of the dijet angular variable χ in different regions of the dijet invariant mass m_{jj} for events with $|y^\star| < 1.7$, $|y_B| < 1.1$ and $p_T > 440$ (50) GeV for the leading (subleading) jets. Shown are the data (points), corrected NLO predictions (solid lines), and examples of the contact interaction (CI) and quantum black hole (QBH) signals [15].

5. Multijet search

In some models of strong gravity, exotic objects such as black holes or string balls can be produced at the LHC. These decay by radiating a number of quarks or gluons, resulting in a final state with many jets with large H_T (defined as the scalar sum of the jet transverse momenta). Events with at least 3 jets with $H_T > 1$ TeV are selected [16], and the H_T distribution is compared to the SM expectation, as shown in figure 13 (left). No evidence for strong gravity effects is observed, and the resulting limits on black hole properties are shown in figure 13 (right).

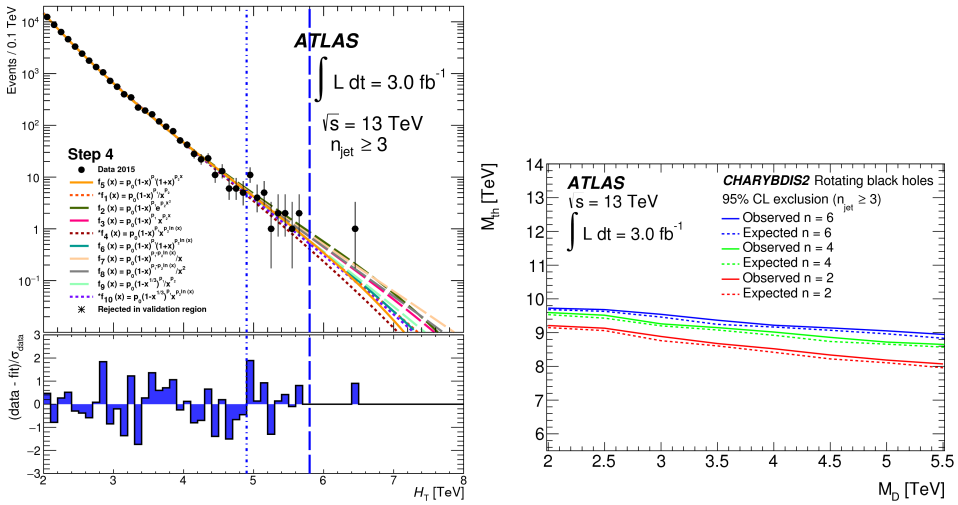

Fig. 13. Left panel: The data in 2.0 TeV $< H_{\mathrm{T}} <$ 4.9 TeV for $n_{\mathrm{jet}} \geq 3$, fitted by the baseline function (solid), and nine alternative functions (dashed). The bottom section of the figure shows the residual significance defined as the ratio of the difference between fit and data over the statistical uncertainty of data, where the fit prediction is taken from the baseline function. Right panel: The observed and expected 95% C.L. exclusion limits on rotating black holes with different numbers of extra dimensions ($n = 2, 4, 6$) in the M_D–M_{th} plane [16].

6. Searches with leptonic final states

The final set of searches reported here are those that look for new phenomena in fully leptonic final states. A typical model to which these searches are sensitive is that of a new heavy vector boson, but in some cases, the searches are sensitive to non-resonant (*i.e.* t-channel) effects as well.

6.1. Search for $W' \to \ell\nu$

A search for $W' \to \ell\nu$ is carried out in both the electron and muon channels [17]. The observed distribution of the transverse mass of the lepton and neutrino is compared to the expectation from SM processes. Good agreement is observed, as shown in figure 14. The resulting limits on the cross section times branching ratio for a W' boson as a function of mass are shown in figure 15.

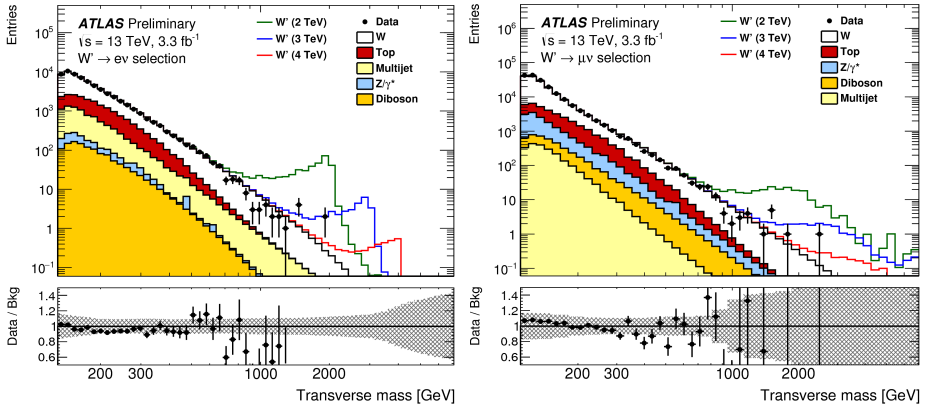

Fig. 14. Transverse mass distributions for events satisfying all selection criteria in the electron (left) and muon (right) channels. The distributions are compared to the sum of all expected backgrounds, with three selected W'_{SSM} signals overlaid. The band in the ratio plot shows the systematic uncertainty [17].

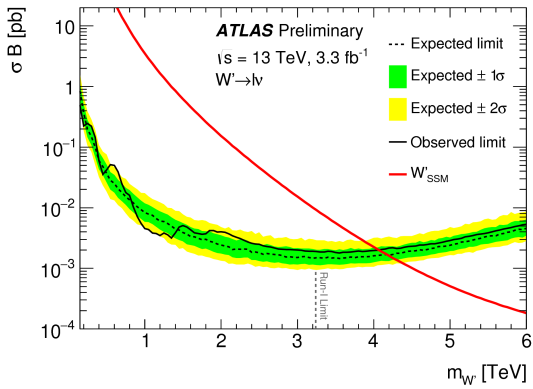

Fig. 15. (Color online) Median expected (black dashed line) and observed (black solid line) 95% C.L. upper limits on cross-section times branching ratio. The predicted σB for W'_{SSM} production is shown by the smoothly falling solid gray (red) line [17].

6.2. Search in the $\ell^+\ell^-$ channel

The $\ell^+\ell^-$ invariant mass distribution could deviate from the SM expectation due either to the presence of a Z' resonance, or the presence of new non-resonant couplings. A search for these effects was performed in both the electron and muon channels, with the $M_{\ell^+\ell^-}$ distributions compared to the SM prediction, as shown in figure 16 [18]. No significant deviations are observed, and the resulting limits on the cross section times branching ratio for a Z' boson as a function of mass are shown in figure 17.

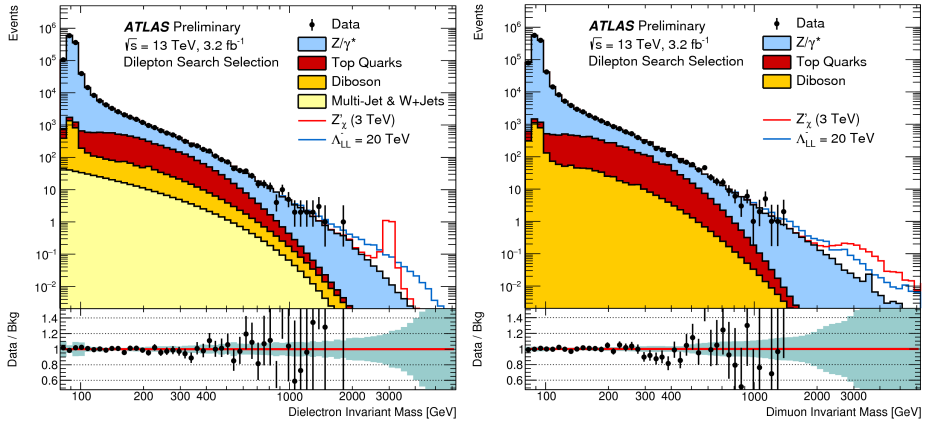

Fig. 16. (Color online) Dielectron (left) and dimuon (right) reconstructed mass distributions after selection, for data and the SM background estimates as well as their ratio. Two selected signals are overlaid. The gray (green) band in the lower panel illustrates the total systematic uncertainty [18].

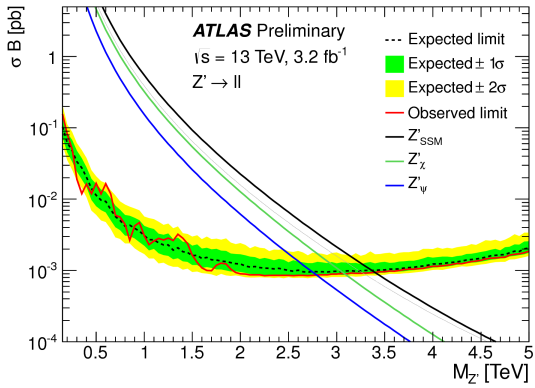

Fig. 17. Upper 95% C.L. limits on the Z' production cross section times branching ratio to two leptons, for the combined electron and muon channels [18].

6.3. Search in the eμ final state

The $e\mu$ final state is particularly sensitive to new physics due to having smaller SM background than the ee or $\mu\mu$ final states. In addition, any resonance observed in this channel would be especially interesting since its decay must violate lepton flavor conservation. A search for such resonance was carried out by comparing the $e\mu$ invariant mass distribution to the SM expectation [19]. Good agreement is observed, and the resulting limits on the cross section times branching ratio for a lepton–flavor-violating Z' as a function of the Z' mass are shown in figure 18.

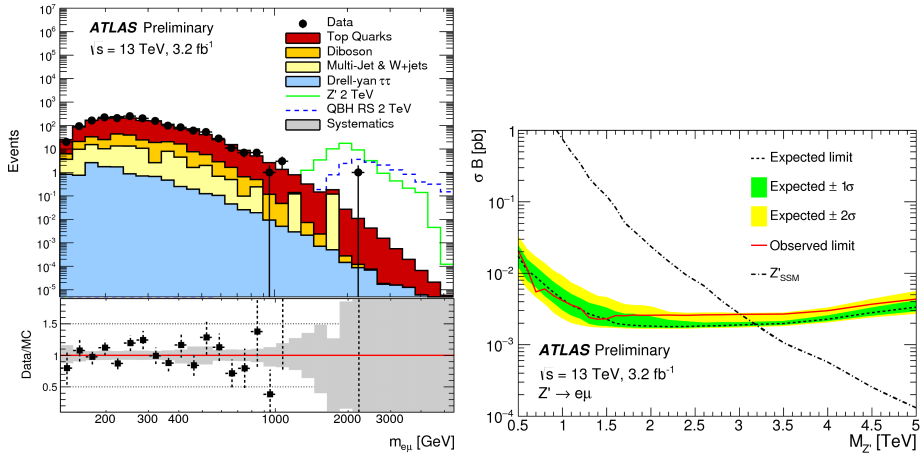

Fig. 18. Left: The invariant mass distribution of selected electron–muon pairs for data and MC expectation. The errors show the statistical uncertainty on the observed yields, while the systematic band includes the addition in quadrature of all systematic uncertainties. Right: The expected and observed 95% C.L. lower mass limits on the Z' production cross section in decays to an $e\mu$ final state [19].

7. Summary

A broad range of searches for exotic phenomena has been carried out using 3.2 fb^{-1} of pp collisions at $\sqrt{s} = 13$ TeV recorded by the ATLAS experiment at the LHC. No evidence of new physics was revealed in these searches, but in 2016 it is expected that ≈ 30 fb^{-1} will be recorded, substantially enhancing the sensitivity to new phenomena.

REFERENCES

[1] ATLAS Collaboration, *JINST* **3**, S08003 (2008).

[2] D. Pappadopulo, A. Thamm, R. Torre, A. Wulzer, *J. High Energy Phys.* **1409**, 060 (2014).

[3] M. Cacciari, G.P. Salam, G. Soyez, *J. High Energy Phys.* **0804**, 063 (2008).

[4] M. Cacciari, G.P. Salam, *Phys. Lett. B* **641**, 57 (2006).

[5] M. Cacciari, G.P. Salam, G. Soyez, *Eur. Phys. J. C* **72**, 1896 (2012).

[6] ATLAS Collaboration, *Eur. Phys. J. C* **76**, 1 (2016).

[7] ATLAS Collaboration, Performance of Jet Substructure Techniques in Early $\sqrt{s} = 13$ TeV pp Collisions with the ATLAS Detector, ATLAS-CONF-2015-035, August 2015.

[8] ATLAS Collaboration, Search for Resonances with Boson-tagged Jets in 3.2 fb^{-1} of pp Collisions at $\sqrt{s} = 13$ TeV Collected with the ATLAS Detector, ATLAS-CONF-2015-073, December 2015.

[9] ATLAS Collaboration, *J. High Energy Phys.* **1512**, 055 (2015).

[10] ATLAS Collaboration, Search for Diboson Resonances in the $\ell\ell qq$ Final State in pp Collisions at $\sqrt{s} = 13$ TeV with the ATLAS Detector, ATLAS-CONF-2015-071, December 2015.

[11] ATLAS Collaboration, Search for WW/WZ Resonance Production in the $\ell\nu qq$ Final State at $\sqrt{s} = 13$ TeV with the ATLAS Detector at the LHC, ATLAS-CONF-2015-075, December 2015.

[12] ATLAS Collaboration, Search for Diboson Resonances in the $\nu\nu qq$ Final State in pp Collisions at $\sqrt{s} = 13$ TeV with the ATLAS Detector, ATLAS-CONF-2015-068, December 2015.

[13] ATLAS Collaboration, Search for New Resonances Decaying to a W or Z Boson and a Higgs Boson in the $\ell\ell b\bar{b}$, $\ell\nu b\bar{b}$, and $\nu\nu b\bar{b}$ Channels in pp Collisions at $\sqrt{s} = 13$ TeV with the ATLAS Detector, ATLAS-CONF-2015-074, December 2015.

[14] ATLAS Collaboration, Search for Dark Matter Produced in Association with a Hadronically Decaying Vector Boson in pp Collisions at $\sqrt{s} = 13$ TeV with the ATLAS Detector at the LHC, ATLAS-CONF-2015-080, December 2015.

[15] ATLAS Collaboration, *Phys. Lett. B* **754**, 302 (2016).

[16] ATLAS Collaboration, *J. High Energy Phys.* **1603**, 026 (2016).

[17] ATLAS Collaboration, Search for New Resonances in Events with One Lepton and Missing Transverse Momentum in pp Collisions at $\sqrt{s} = 13$ TeV with the ATLAS Detector, ATLAS-CONF-2015-063, December 2015.

[18] ATLAS Collaboration, Search for New Phenomena in the Dilepton Final State Using Proton–Proton Collisions at $\sqrt{s} = 13$ TeV with the ATLAS Detector, ATLAS-CONF-2015-070, December 2015.

[19] ATLAS Collaboration, Search for Beyond the Standard Model Phenomena in $e\mu$ Final States in pp Collisions at $\sqrt{s} = 13$ TeV with the ATLAS Detector, ATLAS-CONF-2015-072, December 2015.